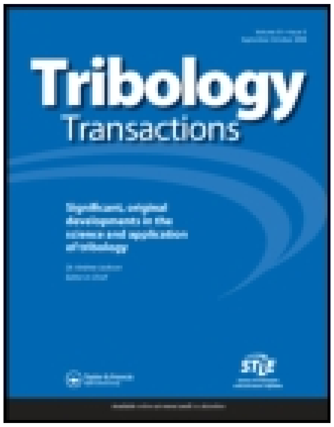

Tribology Transactions
Publication details, including instructions for authors and subscription information:
http://www.tandfonline.com/loi/utrb20

The Influence of the Slip Flow on Steady-State Load Capacity, Stiffness and Damping Coefficients of Elastically Supported Gas Foil Bearings

N. S. Lee [a] , D. H. Choi [a] , Y. B. Lee [b] , T. H. Kim [b] & C. H. Kim [b]

[a] Hanyang University, Department of Mechanical Design and Production Engineering , Seoul, Republic of Korea , 133-791

[b] Korea Institute of Science and Technology, Tribology Research Center , Seoul, Republic of Korea , 136-791

Published online: 25 Mar 2008.

Vol. 45 (2002), 4, 478-484
TRIBOLOGY TRANSACTIONS

The Influence of the Slip Flow on Steady-State Load Capacity, Stiffness and Damping Coefficients of Elastically Supported Gas Foil Bearings©

N. S. LEE and D. H. CHOI
Hanyang University
Department of Mechanical Design and Production Engineering
Seoul, Republic of Korea 133-791
and
Y. B. LEE, T. H. KIM and C. H. KIM
Korea Institute of Science and Technology
Tribology Research Center
Seoul, Republic of Korea 136-791

The slip flow effect is considered to estimate the load capacity and the dynamic coefficients of an elastically-supported gas foil bearing when the local Knudsen number for the minimum film thickness is greater than 0.01. The compressible Reynolds equation with slip flow conditions is used to evaluate the load capacity. The linearized dynamic coefficient equations are obtained by the perturbation method. Numerical predictions compare the static and dynamic force performances considering slip flow at room-to-high temperate with the performance of elastically-supported foil bearing without slip flow for a range of bearing compliances and bearing numbers. It has been shown that the slip flow effect on the load capacity and the dynamic coefficients at high temperature is significant in the region of low bearing numbers.

Presented as a Society of Tribologists and Lubrication Engineers Paper at the ASME/STLE Tribology Conference in Cancun, Mexico October 27-30, 2002
Final manuscript approved August 3, 2002
Review led by Jacqueline Krim

Nomenclature

a	= accommodation coefficient
C_{mn}	= damping coefficients; $m, n = x$ or y
c	= radial clearance
c_f	= foil structural compliance; $c_f = 1/K_f$
c_k	= rarefaction coefficient
D	= bearing diameter
e	= eccentricity
$h, \bar{h}$	= film thickness; $\bar{h} = h/c$
h_n	= nominal film thickness
h_0, h_m	= perturbation component of h; m = x, y, $\dot{x}$ or $\dot{y}$
F_x, F_y	= resultant forces in x and y direction
K_f	= foil structural stiffness per unit area
K_{mn}	= stiffness coefficients; $m,n = x$ or y
Kn	= Knudsen number
Kn_n	= nominal Knudsen number
L	= bearing length
$p, \bar{p}$	= pressure; $\bar{p} = p/p_a$
p_a	= ambient pressure
p_0, p_m	= perturbation component of p; m = x, y, $\dot{x}$ or $\dot{y}$
R	= bearing radius
t	= time variable
$\vec{U}$	= velocity of journal surface
W	= load capacity
w	= foil deflection
z	= axial coordinate
α	= nondimensional compliance; $\alpha = P_a/cK_f$
ΔC	= normalized difference in damping coefficient, $\Delta C = (C_{ns} - C_s)/C_{ns}$
ΔK	= normalized difference in stiffness coefficient, $\Delta K = (K_{ns} - K_s)/K_{ns}$
ΔW	= normalized difference in load capacity, $\Delta W = (W_{ns} - W_s)/W_{ns}$
$\Delta x, \Delta y$	= journal position perturbations
$\Delta \dot{x}, \Delta\dot{y}$	= journal velocity perturbations
ε	= eccentricity ratio
ϕ_0	= attitude angle
γ	= whirl frequency ratio
φ^p	= rarefaction coefficient
λ	= molecular mean free path
θ	= circumferential coordinate
$\Lambda, \vec{\Lambda}$	= bearing number; $\Lambda = (6\mu\omega/p_a)(R/c)^2$, $\vec{\Lambda} = \Lambda\hat{i}$
μ	= fluid viscosity
ω	= journal angular velocity
$\hat{i}$	= unit vector in the θ direction

Subscript

0	= steady state
x	= perturbation x component
y	= perturbation y component
$\dot{x}$	= perturbation $\dot{x}$ component
$\dot{y}$	= perturbation $\dot{y}$ component

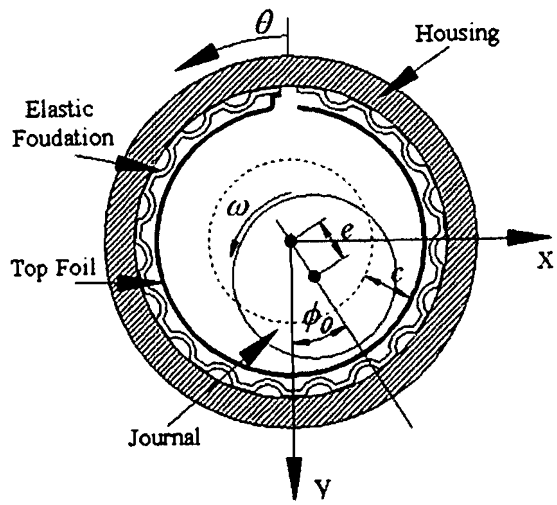

Fig. 1—Elastically supported foil bearing.

KEY WORDS

Foil Air Bearings; Slip Flow; Load-Carrying Capacity; Gas Bearings;

INTRODUCTION

Foil bearings (see Fig. 1) are self-acting compliant-surface hydrodynamic bearings that use ambient air or any process gas as a lubricating fluid. The hydrodynamic film pressure builds up in the small gap between the rotating shaft and the smooth top foil. The top foil provides a smooth bearing surface and is often supported by a series of bump foils that act as springs to make the foil bearings compliant. Because of the compliant bearing surface there are certain advantages over the traditional rigid bearings including higher load capacity for a given minimum film thickness, less power loss, and increased stability. Foil bearings are less susceptible to damage due to large foreign particles in the lubricant flow as the foils can deform instead of seizing. The compliant foil bearings are also more tolerant of misalignment and centrifugal/thermal growth since the compliant foils can accommodate these changes in shaft diameter and bearing clearance.

Because of the high potential of foil bearings, many investigators have analyzed their performance. Heshmat, et al. (1983) first presented an analysis detailing the static performance of bump foil bearings. The Reynolds equation with film thickness coupled to the hydrodynamic pressure was derived. Then, finite difference formulas for these equations were solved using the Newton-Raphson method. Peng and Carpino (1993), (1994), (1997) presented dynamic stiffness and damping coefficients for foil bearings using the perturbation method. The effects of elastic foundation, foil membrane/bending stresses, journal misalignment, and sub-foil Coulomb friction have been analyzed in detail. San Andres, (1995) analyzed the turbulent flow in the foil bearing and included hysteretic damping effects in the form of a complex dynamic stiffness. The effects of excitation frequency and foil structural damping on the dynamic coefficients were investigated.

As the foil bearing has been considered a promising candidate bearing for high-temperature turbomachinery such as the turbocharger and gas turbine engine, a number of experiments at high temperatures were performed. DellaCorte, (1997) measured load capacity and the bearing torque using a high-temperature, high-speed bearing test rig. The results of the experiment concluded that load capacity plotted as a function of shaft speed decreases with temperature. DellaCorte explained that load capacity reduction with temperature most likely occurs due to the stiffness of the bearing support structure decreasing as the temperature increases. Howard, et al. (2001) determined the stiffness and dynamic characteristics of a foil bearing using a high-temperature, optically-based displacement measurement system. Stiffness decreased with temperature by as much as a factor of two from 25°C to 538°C and the damping mechanism shifted from a viscous to a frictional. DellaCorte, et al. (2000) introduced the "Rule of Thumb" (ROT) concept to estimate the foil journal bearing load capacity approximately. The ROT model was validated by the experimental data published in the literature. Howard, (1999) performed a feasibility study of supporting a turbocharger rotor on foil air bearings. It was demonstrated that foil bearings offer a plausible replacement for oil-lubricated bearings in diesel truck turbochargers. Salehi, et al. (2001) presented a thermal analysis of air-lubricated foil bearings based on the simplified energy equation through the Couette Approximation. The Couette Approximation has been found to provide a reasonable tool for the temperature distribution approximation by comparing the experimentally measured temperatures.

According to the test results (DellaCorte, (1997), Howard, et al. (2001)) above, the load capacity, stiffness coefficients, and damping coefficients at high temperatures differ from those at room temperature. Many reasons could explain these differences - changes in clearance and bearing support structure stiffness, damping mechanism shift, increased viscosity of air, etc.

In addition, slip flow also may have an effect on the static and dynamic performance of foil bearings at high temperatures. To explain the slip flow, the Knudsen number (Kn), defined as the ratio of the molecular mean free path (λ) to the film thickness (h), is one important parameter:

$$Kn = \frac{\lambda}{h} \qquad [1]$$

If $Kn < 10^{-2}$, then the fluid is considered a continuum, and the compressible Reynolds equation is used to describe the gas flow. If $10^{-2} < Kn < 10$, then the fluid is considered a rarified gas, and the Reynolds equation with rarefaction coefficients should be used. If $Kn > 10$, then the fluid is considered a free molecular flow.

The rarefaction effect on the foil bearing has been generally ignored because the ratio of the mean free path to the clearance is less than 0.01. But, when the high load is applied to the foil bearing, the local Knudsen number at the minimum film thickness may be greater than 0.01. When the high load is applied at high temperatures, the slip flow effect can be especially large as the molecular mean free path (Gad-el-Hak, (2001)) increases with temperature as shown Fig. 2.

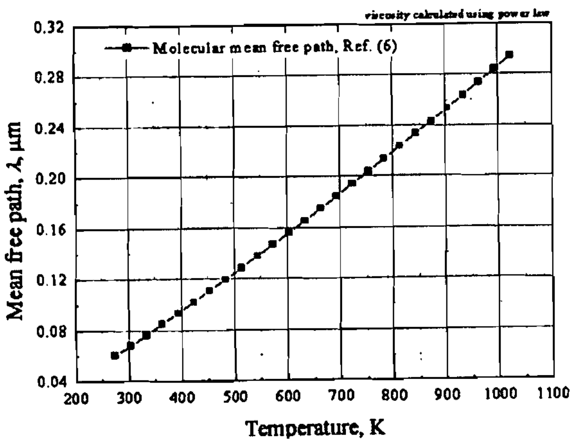

Fig. 2—Molecular mean free path of air *vs*. temperature.

In this paper, the slip flow effect is considered to estimate the load capacity and the dynamic coefficients of an elastically-supported gas foil bearing (see Fig. 1) when the high or allowable load was applied. The modified compressible Reynolds equation with rarefaction effect is used to obtain the load capacity. The linearized dynamic coefficient equations are obtained by the perturbation method. The performance of elastically-supported foil bearings at a higher temperature was compared with those at room temperature with or without rarefaction effect.

ANALYSIS

Governing Equation

In this paper, the lubricant was modeled as an isothermal perfect gas. The pressure distribution within the clearance of the bearing for the coordinate system shown in Fig. 1 was governed as the following modified Reynolds equation.

$$\nabla \cdot \left(-\frac{1}{12\mu}\varphi^p p h^3 \nabla p + \frac{\vec{U}}{2} p h \right) + \frac{\partial}{\partial t}(ph) = 0 \qquad [2]$$

Variables were defined in the nomenclature. $\varphi^p(p,h)$ denotes the molecular rarefaction coefficient in the following form.

$$\varphi^p(p,h) = \sum_{k=0}^{3}\{c_k(p)h^{-k}\} \qquad [3]$$

The rarefaction coefficient, Eq. [3] is valid for high Knudsen numbers using power series expressions in terms of inverse Knudsen number (Fukui, et al. (1990)). A first order slip flow boundary condition (Burgdorfer, (1959)) is one of the approximation equations for thin gas film lubrication and is widely used when the film thickness is greater than 0.1 μm (Mitsuya, et al. (1987)). Because the polished surface roughness of the top foil is normally about 0.2 μm (Walowit, et al. (1973)), the first slip flow boundary condition can be selected without loss of generality. For the first slip approximation, the coefficients c_k can be chosen as $c_0 = 1$, $c_1 = 6a\lambda$, $c_2 = c_3 = 0$. The rarefaction coefficient, Eq. [3] was maintained throughout the theoretical formulation presented here, although it was set to the first order slip boundary condition in results presented later.

This paper focused on the effects of rarefied gas flow on the performance of foil bearings. It was assumed in this formulation that the bending and membrane effect were negligible compared with the elastic foundation and that the structural damping of the elastic foundation was ignored. Using these assumptions, the radial foil structural deflection was related to the pressure in the fluid film by the equation:

$$K_f \cdot w = p - p_a \qquad [4]$$

Perturbation

For small amplitude journal motion measured from the static equilibrium position, the pressure and the film thickness can be expressed as a first order Taylor series:

$$p = p_0 + \Delta p \qquad [5]$$

$$h = h_0 + \Delta h \qquad [6]$$

where

$$\Delta p = p_x \Delta x + p_y \Delta y + p_{\dot{x}} \Delta \dot{x} + p_{\dot{y}} \Delta \dot{y} \qquad [7]$$

$$\Delta h = h_x \Delta x + h_y \Delta y + h_{\dot{x}} \Delta \dot{x} + h_{\dot{y}} \Delta \dot{y} \qquad [8]$$

Substituting the elastic foundation equation for foil defection into the film thickness, the perturbed film thickness for the coordinate system illustrated in Fig. 1 can be expressed as follows:

$$h_x = -sin\theta + c_f p_x \qquad [9]$$

$$h_{\dot{x}} = c_f p_{\dot{x}} \qquad [10]$$

$$h_y = cos\theta + c_f p_y \qquad [11]$$

$$h_{\dot{y}} = c_f p_{\dot{y}} \qquad [12]$$

As the rarefaction coefficient is a function of the pressure and the film thickness, it was expressed as

$$\varphi^p = \varphi^p_o + \left(\frac{\partial \varphi^p}{\partial p}\right)_0 \cdot \Delta p + \left(\frac{\partial \varphi^p}{\partial h}\right)_0 \cdot \Delta h \qquad [13]$$

Substituting Eqs. [5]-[8] into Eq. [2], neglecting the higher-order terms, it yields the zeroth-order and first-order equations. These equations for perturbation in film thickness due to journal displacement can be expressed in the following non-dimensional form:

$$\bar{\nabla} \cdot \left(-\varphi^p_0 \bar{p}_0 \bar{h}^3_o \nabla \bar{p}_o + \vec{\Lambda} \bar{p}_o \bar{h}_o \right) = 0 \qquad [14]$$

$$\bar{\nabla} \cdot \begin{pmatrix} -\varphi^p_0 \bar{p}_0 \bar{h}^3_o \nabla \bar{p}_x - \varphi^p_0 \bar{p}_x \bar{h}^3_o \nabla \bar{p}_0 - 3\varphi^p_0 \bar{p}_0 \bar{h}^2_o \bar{h}_x \nabla \bar{p}_0 \\ -(\partial\varphi^P/\partial p)_0 \bar{p}_x \bar{p}_0 \bar{h}^3_o \nabla \bar{p}_0 - (\partial\varphi^P/\partial\varphi^P/\partial h)_0 \bar{p}_0 \bar{h}^3_o \bar{h}_x \nabla \bar{p}_0 \end{pmatrix}$$

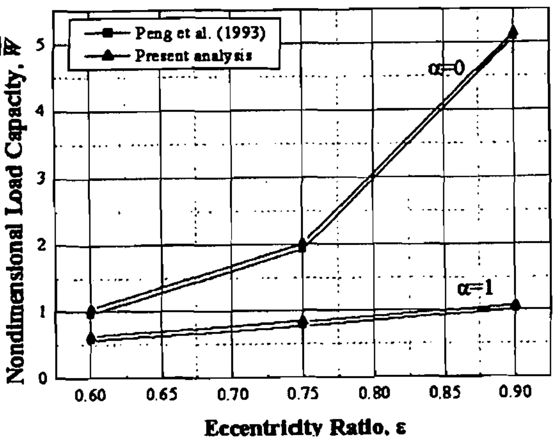

Fig. 3—Effect of bearing compliance on the nondimensional load capacity, L/D=Λ=1.0

$$+\bar{\nabla}\cdot\vec{\Lambda}(\bar{p}_x\bar{h}_o+\bar{p}_o\bar{h}_x)-2\Lambda\gamma(\bar{p}_{\dot{x}}\bar{h}_o+\bar{p}_o\bar{h}_{\dot{x}})=0 \quad [15]$$

$$\bar{\nabla}\cdot\begin{pmatrix} -\varphi_0^p\bar{p}_0\bar{h}_o^3\nabla\bar{p}_{\dot{x}}-\varphi_0^p\bar{p}_{\dot{x}}\bar{h}_o^3\nabla\bar{p}_0-3\varphi_0^p\bar{p}_0\bar{h}_o^2\bar{h}_{\dot{x}}\nabla\bar{p}_0 \\ -(\partial\varphi^P/\partial p)_0\bar{p}_{\dot{x}}\bar{p}_0\bar{h}_o^3\nabla\bar{p}_0-(\partial\varphi^P/\partial\varphi^P/\partial h)_0\bar{p}_0\bar{h}_o^3\bar{h}_{\dot{x}}\nabla\bar{p}_0 \end{pmatrix}$$

$$+\bar{\nabla}\cdot\vec{\Lambda}(\bar{p}_{\dot{x}}\bar{h}_o+\bar{p}_o\bar{h}_{\dot{x}})+2\Lambda\gamma(\bar{p}_x\bar{h}_o+\bar{p}_o\bar{h}_x)=0 \quad [16]$$

$$\bar{\nabla}\cdot\begin{pmatrix} -\varphi_0^p\bar{p}_0\bar{h}_o^3\nabla\bar{p}_y-\varphi_0^p\bar{p}_y\bar{h}_o^3\nabla\bar{p}_0-3\varphi_0^p\bar{p}_0\bar{h}_o^2\bar{h}_y\nabla\bar{p}_0 \\ -(\partial\varphi^P/\partial p)_0\bar{p}_y\bar{p}_0\bar{h}_o^3\nabla\bar{p}_0-(\partial\varphi^P/\partial h)_0\bar{p}_0\bar{h}_o^3\bar{h}_y\nabla\bar{p}_0 \end{pmatrix}$$

$$+\bar{\nabla}\cdot\vec{\Lambda}(\bar{p}_y\bar{h}_o+\bar{p}_o\bar{h}_y)+2\Lambda\gamma(\bar{p}_{\dot{y}}\bar{h}_o+\bar{p}_o\bar{h}_{\dot{y}})=0 \quad [17]$$

$$\bar{\nabla}\cdot\begin{pmatrix} -\varphi_0^p\bar{p}_0\bar{h}_o^3\nabla\bar{p}_{\dot{y}}-\varphi_0^p\bar{p}_{\dot{y}}\bar{h}_o^3\nabla\bar{p}_0-3\varphi_0^p\bar{p}_0\bar{h}_o^2\bar{h}_{\dot{y}}\nabla\bar{p}_0 \\ -(\partial\varphi^P/\partial p)_0\bar{p}_{\dot{y}}\bar{p}_0\bar{h}_o^3\nabla\bar{p}_0-(\partial\varphi^P/\partial h)_0\bar{p}_0\bar{h}_o^3\bar{h}_{\dot{y}}\nabla\bar{p}_0 \end{pmatrix}$$

$$+\bar{\nabla}\cdot\vec{\Lambda}(\bar{p}_{\dot{y}}\bar{h}_o+\bar{p}_o\bar{h}_{\dot{y}})+2\Lambda\gamma(\bar{p}_y\bar{h}_o+\bar{p}_o\bar{h}_y)=0 \quad [18]$$

with the boundary conditions

$$\left.\begin{matrix}\bar{p}=1\\ \bar{p}_x=\bar{p}_{\dot{x}}=\bar{p}_y=\bar{p}_{\dot{y}}=0\end{matrix}\right\} \; at\; z=\pm L/2 \quad [19]$$

$$\left.\begin{matrix}\bar{p}=1\\ \bar{p}_x=\bar{p}_{\dot{x}}=\bar{p}_y=\bar{p}_{\dot{y}}=0\end{matrix}\right\} \; \text{at } \theta=\theta_1, \theta_1+2\pi \quad [20]$$

Equation [14] leads to the steady-state solution for pressure and Eqs. [15] through [18] lead to the solution for the perturbed pressure. Although sub-ambient pressures on the foil do not normally occur since the prevailing ambient pressure underneath the foil will lift it up, no mechanism was provided on this formulation.

Fluid Film Forces and Dynamic Coefficients

With the solutions for steady-state and perturbed pressure, the load capacity and dynamic coefficients can then be obtained by proper integration. Fluid film forces on the foil are calculated by integration of the zeroth-order pressure field on the journal surface.

$$\left\{\begin{matrix}\bar{F}_x\\ \bar{F}_y\end{matrix}\right\}=\frac{1}{p_aR^2}\left\{\begin{matrix}F_x\\ F_y\end{matrix}\right\}=$$

$$\int_{-L/D}^{L/D}\int_0^{2\pi}(\bar{p}-1)\left\{\begin{matrix}sin\theta\\ -cos\theta\end{matrix}\right\}d\theta d\bar{z} \quad [21]$$

The dimensionless load was then given by

$$\bar{W}=\frac{W}{p_aR^2}=\sqrt{\bar{F}_x^2+\bar{F}_y^2} \quad [22]$$

Once the perturbed pressures were known, the stiffness and damping coefficients were readily calculated.

$$\begin{bmatrix}\bar{K}_{xx} & \bar{K}_{xy}\\ \bar{K}_{yx} & \bar{K}_{yy}\end{bmatrix}=\frac{c}{p_aR^2}\begin{bmatrix}K_{xx} & K_{xy}\\ K_{yx} & K_{yy}\end{bmatrix}$$

$$=\int_{-L/D}^{L/D}\int_0^{2\pi}\begin{bmatrix}\bar{p}_x sin\theta & \bar{p}_y sin\theta\\ -\bar{p}_x cos\theta & -\bar{p}_y cos\theta\end{bmatrix}d\theta d\bar{z} \quad [23]$$

$$\begin{bmatrix}\bar{C}_{xx} & \bar{C}_{xy}\\ \bar{C}_{yx} & \bar{C}_{yy}\end{bmatrix}=\frac{c\omega}{p_aR^2}\begin{bmatrix}C_{xx} & C_{xy}\\ C_{yx} & C_{yy}\end{bmatrix}$$

$$=\int_{-L/D}^{L/D}\int_0^{2\pi}\begin{bmatrix}\bar{p}_{\dot{x}} sin\theta & \bar{p}_{\dot{y}} sin\theta\\ -\bar{p}_{\dot{x}} cos\theta & -\bar{p}_{\dot{y}} cos\theta\end{bmatrix}d\theta d\bar{z} \quad [24]$$

Solution Procedure

The steady-state Reynolds equation with the rarefaction coefficient and the dynamic equations were discretized by the control-volume formulation. For the numerical solution of the compressible Reynolds equation, the successive over-relaxation method (Kawabata, (1987)) was used. After the static pressure obtained from Eq. [14] was substituted into Eqs. [15]-[18], the dynamic pressures were obtained by solving the discretized dynamic equations. Thus, dynamic coefficients were obtained from the dynamic pressure with the Eqs. [23] and [24].

RESULTS AND DISCUSSION

The finite difference scheme, with a successive over-relaxation method, was applied to solve the steady-state and perturbed pressure distribution numerically. The accuracy of results was checked by doubling the mesh density. Errors were less than 1 %. Convergence was achieved until 10^{-9} of $\sum|(p_{i,j}^{n+1}-p_{i,j}^n)/p_{i,j}^n|$ was reached. The relaxation factor ranging from 0.1 to 1.0 was used to accelerate the convergence of the solution. In order to check the validity and reliability of the program developed, calcu-

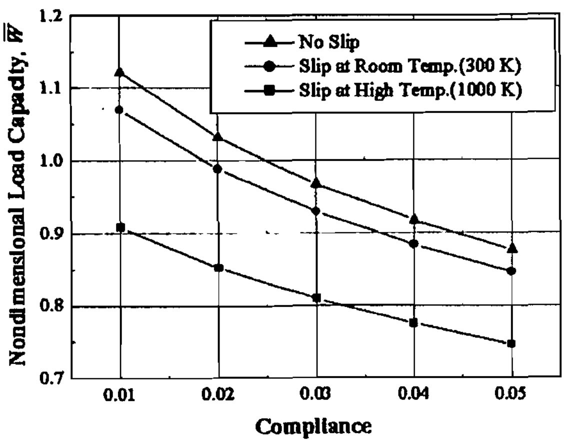

Fig. 4—Comparison of nondimensional load capacity without and with slip flow, L/D=1.0, Λ=0.1, ε=0.95.

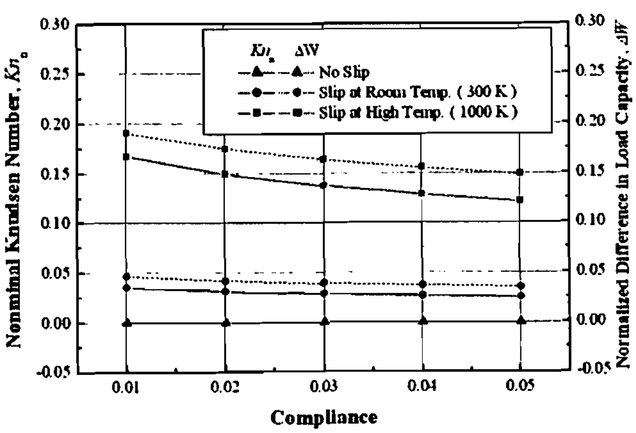

Fig. 5—Comparison of nominal Knudsen number and normalized differences in load capacity without and with slip flow, L/D=1.0, Λ=0.1, ε=0.95.

lations for gas foil bearings from Peng, et al. (1993) were performed. As shown in Fig. 3, the results were in agreement with Peng, et al. Although the rarefaction coefficient, Eq. [3] was maintained throughout the theoretical formulation, the first slip flow boundary condition was selected in this paper. For the first slip approximation, the molecular mean free path in the coefficients c_l was calculated according to Gad-el-Hak, (2001) with accommodation coefficient set to 1.

The non-dimensional forces acting on the journal were calculated from Eq. [21], and the normalized loads were plotted in Fig. 4. The influence of slip flow on the load capacity of foil bearings was greater as the temperature increased. Because the molecular mean free path increases with the temperature, the foil bearing supports less load at the same eccentricity ratio. For the purpose of the present paper, a nominal Knudsen numbers was defined as the ratio of the molecular mean free path to the nominal film thickness which was defined by Heshmat, (1983) as the minimum film thickness along the bearing centerline. And, the normalized difference in load capacity was defined in the nomenclature. In

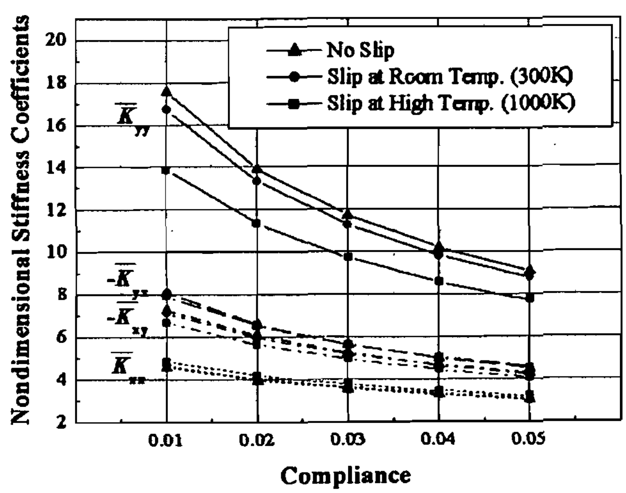

Fig. 6—Comparison of nondimensional stiffness coefficients without and with slip flow, L/D=1.0, Λ=0.1, ε=0.95.

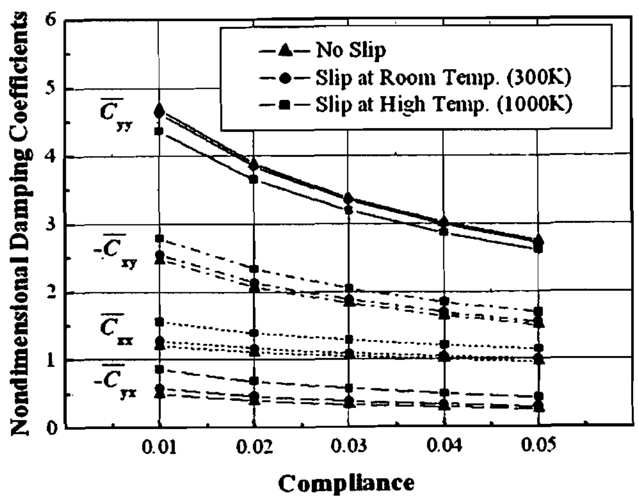

Fig. 7—Comparison of nondimensional damping coefficients without and with slip flow, L/D=1.0, Λ=0.1, ε=0.95.

Fig. 5, this nominal Knudsen numbers and the normalized differences in load capacity were plotted. They were found to decrease with the increases in bearing compliance because the nominal film thickness increases owing to increased deflection of the elastic foundation. Therefore, influence of the slip flow at the given eccentricity ratio reduces with increased bearing compliance.

Figures 6 and 7 show the non-dimensional stiffness and damping obtained from Eqs. [23] and [24], respectively. Generally, the stiffness and damping coefficients for a foil bearing will decrease as the compliance of the bearing increases because of the increased deflection of the foil and elastic foundation. The effect of slip flow on K_{yy} was large compared to the slip flow effect on other stiffness coefficients while the slip flow effect on C_{yy} was comparable to other damping coefficients. As the temperature increased, the stiffness coefficient, K_{yy} and the damping coeffi-

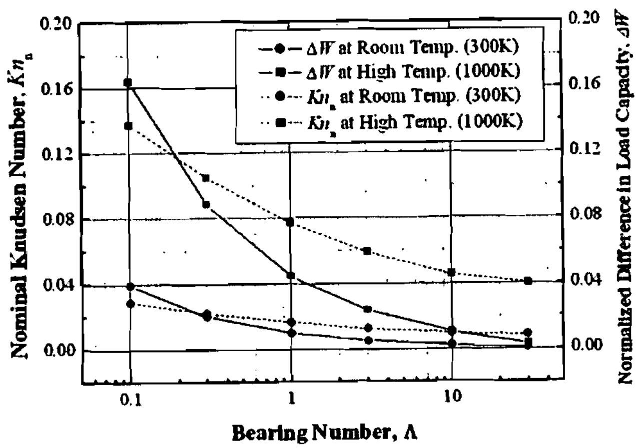

Fig. 8—Comparison of nominal Knudsen number and normalized differences in load capacity without and with slip flow, L/D=1.0, α=0.03, ε=0.95.

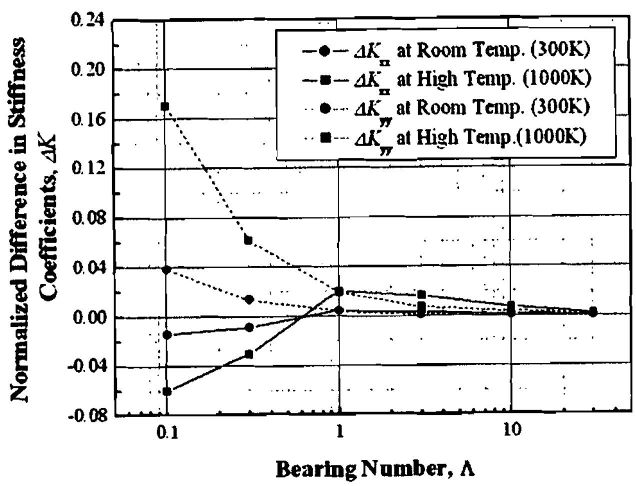

Fig. 9—Comparison of normalized differences in stiffness coefficients without and with slip flow, L/D=1.0, α=0.03, ε=0.95.

cient, C_{yy} were reduced because the load capacity of foil bearing decreased with the increased molecular mean free path.

Figure 8 shows the difference in load capacity and nominal Knudsen number versus bearing numbers ranging from 0.1 to 30. The nominal Knudsen number decreases with the bearing number because the elastic foundation deflects unlike the rigid bearing. The normalized differences in load capacity reduce with bearing number because the Couette flow becomes significant and the nominal Knudsen number decreases at a high bearing number range. The slip flow effect on the load capacity may be ignored in the region of a bearing number greater than 1.0 because the normalized differences in load capacity were less than 0.05 even at the high temperature as shown Fig. 8. Figures 9 and 10 show the normalized differences in direct stiffness coefficients and damping coefficients, which were defined in the nomenclature. The cross-coupled terms of the stiffness and damping coefficients were omitted because the trends of the cross-coupled terms and diagonal terms are the same trends. Like the load capacity, the absolute values of normalized differences in direct stiffness and

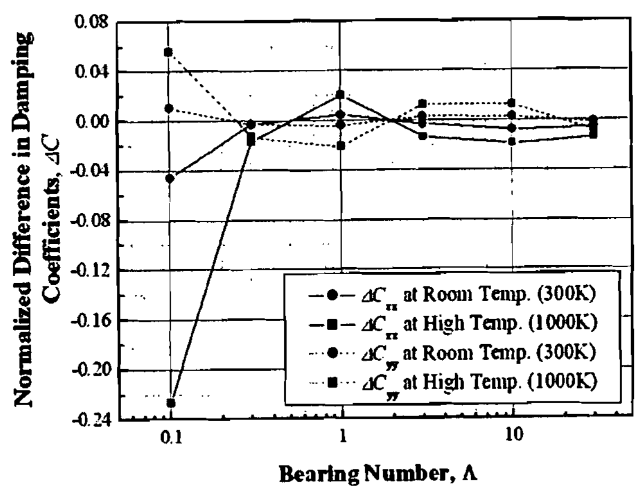

Fig. 10—Comparison of normalized differences in damping coefficients without and with slip flow, L/D=1.0, α=0.03, ε=0.95.

direct damping coefficients were less than 0.05 even at the high temperature when the bearing number was greater than 1.0.

CONCLUSION

The slip flow effect is considered to estimate the load capacity and the dynamic coefficients of an elastically-supported gas foil bearing when the local Knudsen number for a minimum film thickness is greater than 0.01.

At a low bearing number, the influence of the slip flow on the load capacity of foil bearings was greater as the temperature increases because the molecular mean free path increases with the temperature. The normalized differences in load capacity decreased as bearing compliance increased owing to increased deflection of the elastic foundation. As the temperature increased, the stiffness coefficient, K_{yy} and the damping coefficient, C_{yy} decrease because the load capacity of the foil bearing decreases with the increased molecular mean free path.

At a high bearing number, the normalized differences in load capacity and the absolute values of normalized differences in dynamic coefficients decreased because the Couette flow became significant and the elastic foundation deflected. Even at a higher temperature, these values in load capacity and dynamic coefficients were less than 0.05 when the bearing number was greater than 1.0. Therefore, the slip flow at a bearing number greater than 1.0 may be ignored.

ACKNOWLEDGMENT

This work was supported by a grant from the Critical Technology 21 Project of the Ministry of Science and Technology, Korea.

REFERENCES

(1) Burgdorfer, A. (1959), "The Influence of the Molecular Mean Free Path on the Performance of Hydrodynamic Gas Lubricated Bearings," *ASME Jour. of Basic Eng.*, **81**, pp 94-100.

(2) Carpino, M., Peng, J. and Medvetz, L. (1994), "Misalignment In A Complete Shell Gas Foil Journal Bearing," *Trib. Trans.*, **37**, pp 829-835.

(3) DellaCorte, C. (1997), "A New Foil Air Bearing Test Rig for Use to 700°C and 70,000 rpm," **NASA TM-107405**, NASA, Cleveland, OH.
(4) DellaCorte, C. and Valco, M. J., (2000), "Load Capacity Estimation of Foil Air Journal Bearings for Oil-Free Turbomachinery Application," in *Proc. ASME/STLE Trib. Conf. in Seattle, Washington*, Preprint No. **00-TC-4**.
(5) Fukui, S. and Kaneko, R. (1990), "A Database for Interpolation of Poiseuille Flow Rates for High Knudsen Number Lubrication Problems," *ASME Jour. of Trib.*, **112**, pp 78-83.
(6) Gad-el-Hak, M. (2001), *The MEMS Handbook*, CRC Press, Florida.
(7) Heshmat, H., Walowit, J. A. and Pinkus, O. (1983), "Analysis of Gas Lubricated Foil Journal Bearings," *ASME Jour. of Lubr. Tech.*, **105**, pp 647-655.
(8) Howard, S. A., DellaCorte, C., Valco, M. J., Prahl, J. M. and Heshmat, H. (2001), "Dynamic Stiffness and Damping Characteristics of a High Temperature Air Foil Journal Bearing," in *Proc. STLE/ASME Trib. Conf. in San Francisco, California*, Preprint No. **01-TC-7**.
(9) Howard, S. A. (1999), "Rotordynamics and Design Methods of an Oil-Free Turbocharger," **NASA/CR-1999-208689**, NASA, Cleveland, OH.
(10) Kawabata, N. (1987), "Numerical Analysis of Reynolds Equation for Gas Lubrication in a High L Region," *JSME Int. Jour.*, **30**, pp 836-842.
(11) Mitsuya, Y. and Ohkubo, G. (1987), "High Knudsen Number Molecular Rarefaction Effects in Gas-Lubricated Slider Bearings for Computer Flying Heads," *ASME Jour. of Trib.*, **109**, pp 276-282.
(12) Peng, J. and Carpino, M. (1993), "Calculation of Stiffness and Damping Coefficients for Elastically Supported Gas Foil Bearings," *ASME Jour. of Trib.*, **115**, pp 20-27.
(13) Peng, J. and Carpino, M. (1997), "Finite Element Approach to the Prediction of Foil Bearing Rotor Dynamic Coefficients," *ASME Jour. of Trib.*, **119**, pp 85-90.
(14) Salehi, M., Swanson, E. and Heshmat, H. (2001), "Thermal Features of Compliant Foil Bearings-Theory and Experiments," *ASME Jour. of Trib.*, **123**, pp 566-571.
(15) San Andres, L. (1995), "Turbulent Flow Foil Bearings for Cryogenic Applications," *ASME Jour. of Trib.*, **117**, pp 185-195.
(16) Walowit, J. A., McCabe, J. T., Moyer, T., Murry, S. F. and Arwas, E. B. (1973), "Gas Lubricated Foil Bearing Technology Development for Propulsion and Power Systems," **NASA AFAPL-TR-73-92**.